8. Experiments with ^{13}C- or ^{15}N-labeled RNA were performed on 500- or 600-MHz NMR instruments at the Francis Bitter National Magnet Laboratory or a Varian Unity-Plus 750-MHz instrument. A three-dimensional NOESY-HSQC [G. M. Clore, A. Bax, P. C. Driscoll, P. T. Wingfield, A. M. Gronenborn, *Biochemistry* **29**, 8172 (1990)] (τ_M = 200 ms), a four-dimensional HMQC-NOESY-HSQC [G. W. Vuister *et al.*, *J. Magn. Reson. B* **101**, 210 (1993)] (τ_M = 150 ms), and a two-dimensional double-half-filter NOESY experiment [G. Otting and K. Wuthrich, *Q. Rev. Biophys.* **23**, 39 (1990)] (τ_M = 200 ms) with ^{13}C-labeled RNA and expressed Rev peptide were performed to obtain NOEs for molecular modeling. A three-dimensional NOESY-HSQC [S. Mori, C. Abeygunawardana, M. O. Johnson, P. C. M. v. Zijl, *J. Magn. Reson. B* **108**, 94 (1995)] (τ_M = 150 ms) with ^{15}N-labeled RNA was also obtained.
9. M. Nilges, G. M. Clore, A. M. Gronenborn, *FEBS Lett.* **229**, 317 (1988).
10. Molecular modeling was performed with the DGII and DISCOVER modules of Insight II (Biosym). The force constants for NMR-derived distance and torsion restraints were 10 kcal mol^{-1} Å^{-2} and 60 kcal mol^{-1} degree^{-2}, respectively. No nonexperimental torsion restraints were used to enforce A-form geometry for any region of the RNA. A quartic repulsive function was used for nonbonding contacts in all calculations, and electrostatic interactions were completely neglected. A total of 140 distance geometry structures were generated and input into a high-temperature (1000 K) simulated-annealing protocol using the AMBER forcefield with the masses for all the atoms set to 100 [A. T. Brunger, *X-PLOR User Manual, Version 3.1* (Yale Univ. Press, New Haven, CT, 1992)]. The force constants for the covalent geometry, distance and dihedral, and nonbonded terms were sequentially scaled from 1% to full value over 36 ps of dynamics in 3-fs steps. The temperature was then cooled to 10 K over 21 ps. The 30 structures with the lowest NMR restraint violation energies were chosen for further refinement. Peptide hydrogen bonds were added for the well-defined α helix at this stage. The refinement protocol consisted of 6 ps of dynamics (1-fs steps) at 500 K, scaling the nonbonded terms from 10% to full value. The temperature was then exponentially cooled to 10 K over 9 ps, followed by 100 and 500 steps of steepest and conjugate gradient minimization, respectively. The 19 structures with the lowest restraint violation energies and no violations >0.3 Å were chosen for detailed structural analysis. An average structure (SA) was generated by superimposing the coordinates of all 19 structures and then averaging the coordinates. The covalent geometry of the average structure was regularized by 100 steps of steepest descent and 500 steps of conjugate gradient minimization.
11. R. Tan and A. Frankel, *Biochemistry* **33**, 14579 (1994).
12. C. O. Pabo and R. T. Sauer, *Annu. Rev. Biochem.* **61**, 1053 (1992).
13. K. M. Weeks and D. M. Crothers, *Science* **261**, 1574 (1993).
14. The major groove width of the RNA was quantitated by measuring the shortest phosphorus atom distances across the groove and subtracting 5.8 Å for the van der Waals radii of the phosphate group.
15. D. P. Bartel, M. L. Zapp, M. R. Green, J. W. Szostak, *Cell* **67**, 529 (1991).
16. S. Iwai, C. Pritchard, D. A. Mann, J. Karn, M. J. Gait, *Nucleic Acids Res.* **20**, 6465 (1992).
17. J. Kjems, B. J. Calnan, A. D. Frankel, P. A. Sharp, *EMBO J.* **11**, 1119 (1992).
18. C. E. Pritchard *et al.*, *Nucleic Acids Res.* **22**, 2592 (1994).
19. E. T. Harper and G. D. Rose, *Biochemistry* **32**, 7605 (1993).
20. P. C. Lyu and D. E. Wemmer, *ibid.*, p. 421; A. M. Gronenborn and G. M. Clore, *J. Biomol. NMR* **4**, 455 (1994).
21. J. D. Puglisi, L. Chen, S. Blanchard, A. D. Frankel, *Science* **270**, 1200 (1995); X. Ye, R. A. Kumar; D. J. Patel, *Chem. Biol.* **2**, 827 (1995).
22. L. Chen and A. D. Frankel, *Proc. Natl. Acad. Sci. U.S.A.* **92**, 5077 (1995); R. Tan and A. D. Frankel, *ibid.*, p. 5282; K. Harada, S. A. Martin, A. D. Frankel, *Nature* **380**, 175 (1996).
23. M. A. Rould, J. J. Perona, D. Söll, T. A. Steitz, *Science* **246**, 1135 (1989); M. Ruff *et al.*, *ibid.* **252**, 1682 (1991); V. Biou, A. Yaremchuk, M. Tukalo, S. Cusack, *ibid.* **263**, 1404 (1994).
24. J. D. Puglisi, R. Tan, B. J. Calnan, A. D. Frankel, J. R. Williamson, *ibid.* **257**, 76 (1992); J. D. Puglisi, L. Chen, A. D. Frankel, J. R. Williamson, *Proc. Natl. Acad. Sci. U.S.A.* **90**, 3680 (1993).
25. J. P. Staley and P. S. Kim, *Protein Sci.* **3**, 1822 (1994); T. N. M. Schumacher *et al.*, *Science* **271**, 1854 (1996).
26. J. L. Battiste, data not shown.
27. R. D. Peterson *et al.*, *Biochemistry* **33**, 5357 (1994).
28. S. M. Pascal, D. R. Muhandiram, T. Yamazuki, J. D. Forman-Kay, L. E. Kay, *J. Magn. Reson. B* **103**, 197 (1994).
29. J. L. Battiste, R. Tan, A. D. Frankel, J. R. Williamson, *Biochemistry* **33**, 2741 (1994).
30. T. E. Ellenberger *et al.*, *Cell* **71**, 1223 (1992).
31. We thank J. Puglisi for helpful discussions, C. Turner and A. Brodsky for assistance with NMR experiments, M. Milhollen and P. Kim for providing the pMM and pTM plasmids, M. Oakley and C. Cilley for assistance in purification of peptides, and C. Pabo for critical comments. J.L.B. was supported in part by the NIH Interdepartmental Biotechnology Program (GM-08344), and R.T. is a Scholar for the American Foundation for AIDS Research (70405-15-RF). Supported by grants from the National Sciences and Engineering Research Council of Canada (L.E.K.), the Medical Research Council of Canada (L.E.K.), the Searle Scholars Program of the Chicago Community Trust (J.R.W.), and NIH grants GM-39589 (A.D.F. and J.R.W.) and GM-53320 (J.R.W.).

26 June 1996; accepted 15 August 1996

Regulation of Integrin Function by the Urokinase Receptor

Ying Wei, Matvey Lukashev, Daniel I. Simon, Sarah C. Bodary, Steven Rosenberg, Michael V. Doyle, Harold A. Chapman*

Integrin function is central to inflammation, immunity, and tumor progression. The urokinase-type plasminogen activator receptor (uPAR) and integrins formed stable complexes that both inhibited native integrin adhesive function and promoted adhesion to vitronectin via a ligand binding site on uPAR. Interaction of soluble uPAR with the active conformer of integrins mimicked the inhibitory effects of membrane uPAR. Both uPAR-mediated adhesion and altered integrin function were blocked by a peptide that bound to uPAR and disrupted complexes. These data provide a paradigm for regulation of integrins in which a nonintegrin membrane receptor interacts with and modifies the function of activated integrins.

Receptors of the integrin family mediate adhesion of cells to extracellular matrices as well as intercellular interactions, and modulate transduction of regulatory signals that are central to inflammation, immunity, hemostasis, and tumor progression. In mediating these functions, integrin receptors undergo regulated and reversible activation as a result of ligand binding or cellular stimulation by chemoattractants (*1*). Activation is characterized by conformational changes in the integrin extracellular domains, reorganization of intracytoplasmic connections, and redistribution of integrins on the cell surface, which together augment integrin avidity for ligands (*2*). Dynamic activation of integrins is central to integrin-mediated adhesion and migration (*1*), although little is known about functionally important interactions of integrins with other membrane proteins that might regulate this process. We have now identified a pathway of interaction between activated integrins and a nonintegrin receptor that regulates integrin function.

The urokinase receptor (uPAR) is a glycosyl-phosphatidylinositol (GPI)–linked cell surface protein that is expressed in many cell types and is spatially and temporally associated with cellular structures that regulate cell adhesion, migration, and invasion (*3*). Previously, we have shown that uPAR can function as an adhesion receptor for vitronectin, with the vitronectin binding site being distinct from the urokinase binding site (*4*, *5*). uPAR colocalizes with integrins in focal contacts, at the leading edge of migrating cells, and in antibody-induced clusters (*6*). The receptor copurifies with and influences the function of the leukocyte integrin Mac-1, suggesting that it interacts functionally with this integrin (*7*). We hypothesized that formation of complexes between uPAR, which does not contain a transmembrane domain, and integrins might provide an integrin-mediated link between uPAR and the cytoskeleton

Y. Wei, D. I. Simon, H. A. Chapman, Department of Medicine, Brigham and Women's Hospital and Harvard Medical School, Boston, MA 02115, USA.
M. Lukashev, Department of Stomatology, University of California, San Francisco, CA 94143, USA.
S. C. Bodary, Genentech, South San Francisco, CA 94080, USA.
S. Rosenberg and M. V. Doyle, Chiron Corporation, Emeryville, CA 94608, USA.

*To whom correspondence should be addressed at Brigham and Women's Hospital, Room 703, Thorn Research Building, 20 Shattuck Street, Boston, MA 02115, USA.

and promote adhesion.

Human embryonic kidney 293 cells were transfected with uPAR cDNA. The transfected cells displayed markedly enhanced adhesion to vitronectin (Fig. 1A) (*5*). Expression of uPAR also markedly inhibited β1-integrin–dependent adhesion to fibronectin (Fig. 1A). Both the enhanced adhesion to vitronectin and suppressed adhesion to fibronectin were reversed by treatment of transfectants with phosphatidylinositol-specific phospholipase C (PI-PLC), which removes most of the GPI-anchored uPAR (Fig. 1A) (*5*, *8*). Expression of uPAR in 293 cells had no detectable effect on cell surface expression of β1-integrins (*9*), supporting the view that uPAR expression alters the adhesive phenotype of cells by regulating integrin function.

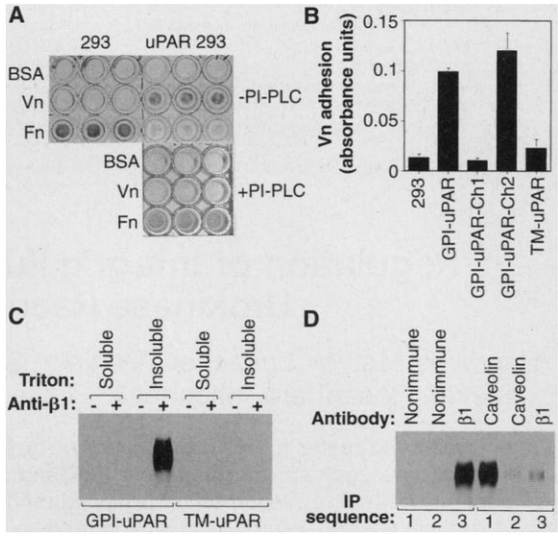

Fig. 1. Interaction of uPAR with β1-integrins and caveolin. (**A**) Adhesion properties of control 293 cells and 293 cells transfected with GPI-uPAR cDNA (uPAR 293). Expression of GPI-uPAR promoted stable adhesion to vitronectin (Vn) and inhibited adhesion to fibronectin (Fn). Treatment of the uPAR transfectants with PI-PLC to release GPI-uPAR reversed the adhesive phenotype (*8*). BSA, bovine serum albumin. (**B**) Adhesion of 293 cells to vitronectin. Cell clones expressing full-length (Ch1) or truncated (Ch2) β1-integrin cytoplasmic tails prepared as in (*10*) were transfected with GPI-uPAR cDNA and selected as in (*5*). Chimera expression was induced by cadmium for 6 hours before assaying for adhesion to vitronectin at 37°C. A construct (TM-uPAR) consisting of the extracellular domain of uPAR and the transmembrane and cytoplasmic domains of IL-2Rα was prepared as described (*12*). Vitronectin was adsorbed onto plastic 96-well tissue culture plates, and the extent of cell adherence after vigorous washing was determined as in (*5*). Data are means ± SD (n = 3). (**C**) Immunoprecipitation of uPAR with antibodies to β1-integrin. Triton X-100–soluble and –insoluble fractions of cell lysates, prepared as in (*11*), were subjected to immunoprecipitation with antibodies to β1-integrin (anti-β1), and the precipitates were analyzed by immunoblotting with antibodies to uPAR. Both rabbit polyclonal antibodies specific for the cytoplasmic tail of the β1 subunit (shown) and a rat monoclonal antibody that inhibits ligand binding to β1-integrins (not shown) coprecipitated GPI-uPAR. (**D**) Depletion of β1-integrin–uPAR complexes with antibodies to caveolin. Triton-insoluble extracts of GPI-uPAR transfectants were solubilized in RIPA buffer and twice subjected to immunoprecipitation (IP) with antibodies to caveolin, in order to deplete caveolin, or with nondepleting, nonimmune antibodies. β1-Integrins were then immunoprecipitated and all precipitates were subjected to immunoblot analysis with antibodies to uPAR.

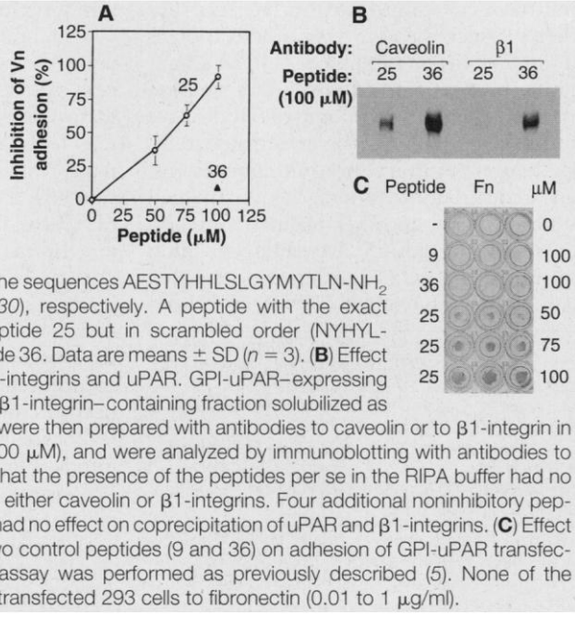

Fig. 2. Requirement of association of β1-integrins with uPAR for adhesion to vitronectin. (**A**) Effect of phage display peptides on adhesion of GPI-uPAR–expressing cells to vitronectin. GPI-uPAR–expressing 293 cells were suspended and adhesion to vitronectin in the presence of various peptide concentrations was assessed after 1 hour. Peptides 25 and 36 contain 17 amino acids with the sequences AESTYHHLSLGYMYTLN-NH_2 and AEPHTAIYYYLPHFSQM-NH_2 (*30*), respectively. A peptide with the exact composition of amino acids of peptide 25 but in scrambled order (NYHYL-ESSMTALYTLGH) behaved as peptide 36. Data are means ± SD (n = 3). (**B**) Effect of peptides on coprecipitation of β1-integrins and uPAR. GPI-uPAR–expressing 293 cells were lysed, and the uPAR–β1-integrin–containing fraction solubilized as described (*11*). Immunoprecipitates were then prepared with antibodies to caveolin or to β1-integrin in the presence of peptide 25 or 36 (100 μM), and were analyzed by immunoblotting with antibodies to uPAR. Control experiments verified that the presence of the peptides per se in the RIPA buffer had no effect on the immunoprecipitation of either caveolin or β1-integrins. Four additional noninhibitory peptides from the peptide library screen had no effect on coprecipitation of uPAR and β1-integrins. (**C**) Effect of peptide 25 (50 to 100 μM) and two control peptides (9 and 36) on adhesion of GPI-uPAR transfectants to fibronectin. The adhesion assay was performed as previously described (*5*). None of the peptides promoted adhesion of nontransfected 293 cells to fibronectin (0.01 to 1 μg/ml).

In contrast to the adhesion of control 293 cells, adhesion of the uPAR transfectants to vitronectin was blocked only by antibodies to uPAR and not by antibodies to β1- or β5-integrins (*5*). To determine whether uPAR- and integrin-mediated adhesion share a common cytoplasmic mechanism, we engineered uPAR transfectants to coexpress a chimeric protein comprised of β1-integrin transmembrane and cytoplasmic domains fused with the extracellular domain of mouse CD4. Expression of this chimera specifically blocks integrin function in a dominant negative manner, presumably by disrupting interactions of integrins with cytoplasmic components (*10*). Expression of a control CD4–β1-integrin construct lacking the integrin cytoplasmic tail (uPAR-Ch2), which does not inhibit integrin function, had no effect on uPAR-mediated adhesion (Fig. 1B). In contrast, coexpression of the β1-integrin cytoplasmic domain construct (uPAR-Ch1) completely blocked adhesion to vitronectin, confirming the interdependence of uPAR and integrin function in these cells.

The activity of uPAR as an adhesion receptor mirrored its ability to form stable complexes with integrins, as demonstrated by immunoprecipitation. Intact GPI-uPAR formed complexes with β1-integrins, which were associated with the Triton X-100–insoluble subcellular fraction (Fig. 1C) (*11*). In contrast, a construct (TM-uPAR) comprising the extracellular domain of uPAR and the transmembrane and cytoplasmic domains of the interleukin-2 receptor α chain (IL-2Rα), which lacked the ability to mediate cell adhesion (Fig. 1B), showed little or no association with integrins (Fig. 1C) (*12*). GPI-uPAR was readily detected in the β1-integrin immunoprecipitates by immunoblot analysis. However, virtually no uPAR signal was apparent when identical material immunoprecipitated with antibodies to β1-integrin from lysates of cells labeled with [^{35}S]methionine and [^{35}S]cysteine was analyzed by autoradiography, suggesting that β1-integrin–uPAR complexes represent only a small proportion of the total β1-integrin pool. Several GPI-anchored proteins, including uPAR, associate with plasma membrane structures termed caveolae, which contain caveolin, a protein associated with intracellular signaling pathways and cytoskeletal elements (*13*). When the Triton X-100–insoluble fractions of GPI-uPAR transfectants were

first immunodepleted of caveolin, the amount of uPAR in the β1-integrin immunoprecipitates decreased markedly (Fig. 1D). Therefore, uPAR-mediated adhesion to vitronectin correlates with the formation of multimeric membrane complexes of integrins, caveolin, and uPAR itself.

To examine further the importance of the physical association between uPAR and integrins for the ability of uPAR to mediate adhesion and regulate integrin function, we attempted to disrupt uPAR-integrin complexes in intact cells. A bacteriophage peptide display library was screened for uPAR-binding phages to identify potential peptide inhibitors of uPAR-integrin interactions. The screen selected for peptides that bound to uPAR but did not interfere with the binding of uPAR to vitronectin or urokinase. One of the isolated phages displayed such a peptide (*14*). This peptide (peptide 25) and several controls were synthesized, purified, and screened for their effects on adhesion. Peptide 25, but not control peptides, inhibited GPI-uPAR–dependent adhesion of 293 cells to vitronectin; the median inhibitory concentration (IC_{50}) was ~60 μM (Fig. 2A). Peptide 25 had no effect on the adhesion of nontransfected 293 cells to fibronectin. Immunoprecipitation experiments showed that peptide 25, but not several control peptides, disrupted integrin-caveolin-uPAR complexes at a concentration that blocked adhesion (Fig. 2B). Moreover, peptide 25 restored the adhesion of GPI-uPAR transfectants to fibronectin (Fig. 2C). The restored fibronectin adhesion was again inhibited by antibodies to β1-integrin. These results confirm that the uPAR-integrin-caveolin complex represents a functional unit that mediates uPAR-dependent cell adhesion and modifies integrin function.

Whereas only GPI-uPAR–expressing 293 cells showed enhanced adhesion to vitronectin, both GPI-uPAR– and TM-uPAR–expressing cells showed reduced adhesion to fibronectin. Thus, whereas the GPI anchor may be critical for complex formation with integrins and uPAR-dependent adhesion, the extracellular domain of uPAR alone may be capable of interacting with and modifying the function of integrins. To investigate this possibility, we performed fibronectin adhesion assays with nontransfected 293 cells in the presence of recombinant soluble uPAR (suPAR) (*15*). suPAR is unable to mediate cell adhesion to vitronectin, and previous studies have shown that cells expressing this form of the receptor have little or no suPAR stably associated with them after washing (*5*). Exposure of 293 cells to recombinant suPAR inhibited adhesion to fibronectin and collagen (Cl) in a dose-dependent manner (Fig. 3A). The inhibitory effect of suPAR was reversible with the addition of monoclonal antibodies to uPAR (R4, 5 μg/ml), but not of control antibodies, confirming the specificity of this effect.

Because uPAR markedly altered the adhesive phenotype of 293 cells, the ability of uPAR to affect haptotactic migration was also examined. GPI-uPAR transfectants migrated across porous filters onto vitronectin at a markedly higher rate than nontransfected 293 cells (20% of total cells versus 0.4%) over 24 hours, whereas fewer transfectants than control cells migrated toward fibronectin (0.8 versus 33%) (*16*). Similarly, the addition of recombinant baculovirus suPAR (100 nM) inhibited the migration of nontransfected 293 cells onto fibronectin by >75%. These results mirror the altered patterns of adhesion (Figs. 1A and 3A). The inhibitory effects of uPAR were not limited to the 293 cell model. Vascular smooth muscle cells from passages 1 to 3 were allowed to migrate in the presence of suPAR (*17*). Integrins mediate the binding and migration of human smooth muscle cells on fibronectin (*18*). Recombinant suPAR markedly impaired both spreading of vascular smooth muscle cells and their haptotactic migration onto fibronectin (Fig. 3B). Thus, uPAR appears capable of affecting integrin function in various cell types.

The fact that uPAR markedly alters adhesion and migration without altering integrin surface expression suggests that uPAR may affect the function of activated integrins. This possibility was explored by measuring the binding of fibronectin to 293 cells in the presence of suPAR (*19*). Neither suPAR nor GPI-uPAR had any discernible effect on RGD (Arg-Gly-Asp)–sensitive binding of fibronectin to 293 cells at 4°C, as would be expected if uPAR effectively interacts only with activated integrins [activation by ligand requires metabolic energy, which would not be available at 4°C (*2*)]. Experiments were therefore performed in the presence of the monoclonal antibody TS2/16, which directly induces the activated conformation of β1-integrins (*20*). In the presence of TS2/16, suPAR markedly inhibited fibronectin binding (Fig. 3C). Consistent with these observations, the inhibitory effects of suPAR on adhesion shown in Fig. 3A were not reversed, but were actually enhanced, by the addition of TS2/16 (3 μg/ml) to the adhesion assays. These results demonstrate that the inhibitory effects of uPAR on β1-integrin function are promoted by, and may require, integrin activation.

We further examined this concept by investigating whether suPAR interacts with other integrins in an activation-dependent

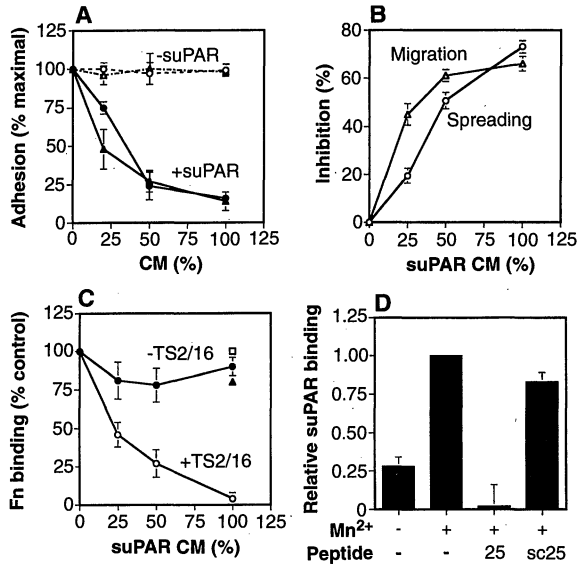

Fig. 3. Interaction of suPAR with integrins. (**A**) Inhibition by suPAR of 293 cell adhesion to fibronectin and collagen. suPAR-conditioned medium (solid symbols) and control conditioned medium (open symbols) were prepared as described (*5*) and tested for their effects on adhesion of 293 cells to fibronectin (circles) or collagen (triangles). In all instances, adhesion could be blocked by antibodies to β1-integrin. suPAR had no effect on adhesion of the cells to polylysine. CM, conditioned medium. (**B**) Inhibition by suPAR of the spreading (○) and migration (△) of vascular smooth muscle cells. Suspended cells were allowed to settle onto surfaces coated with fibronectin (1 μg/ml) at 37°C for 15 to 30 min, after which spread cells were counted under phase-contrast microscopy. Overnight migration of cells across porous filters was assessed as described (*16*). (**C**) Inhibition by suPAR of ligand binding by activated integrins. Suspended 293 cells were incubated in the absence (●) or presence (○) of the monoclonal antibody TS2/16 (3 μg/ml) at 4°C for 30 min, and the binding of ^{125}I-labeled fibronectin (5 nM) was then determined in the presence of various amounts of suPAR-conditioned medium. Specific fibronectin binding was increased by ~25% by TS2/16 in the absence of suPAR. Conditioned medium without suPAR had no effect on fibronectin binding either in the presence (□) or absence (▲) of TS2/16. (**D**) Interaction of suPAR with Mac-1. Mac-1 (250 ng/ml) was immobilized in microtiter wells, and nonspecific sites were blocked with BSA (5 mg/ml). Biotinylated suPAR (100 nM) was added in the presence of either $CaCl_2$ and $MgCl_2$ or $MnCl_2$ as indicated, the plate was incubated for 90 min at 25°C, and bound suPAR was quantified. Peptide 25 or a scrambled version of this peptide (sc25) was added to the binding assays at a final concentration of 100 μM. All data are means ± SD (n = 3).

manner. In myelomonocytic cells, uPAR interacts with the β2-integrin CD11b/CD18 (Mac-1) (*7*). Human monocytic THP-1 cells bind and degrade soluble fibrinogen in a Mac-1–dependent manner (*21*). This binding and degradation was inhibited by recombinant suPAR with an IC_{50} of ~95 nM. The β2-integrin–specific activating monoclonal antibody KIM 127 (10 μg/ml) markedly potentiated inhibition by suPAR, reducing the IC_{50} to 0.1 nM (*22*). We next investigated whether suPAR would directly bind to highly purified Mac-1 (*23*) in an activation-dependent manner. Purified Mac-1 retains an active conformation when plated onto plastic in the presence of manganese (*24*). Biotinylated suPAR bound to immobilized Mac-1 and binding was enhanced by activation with manganese (Fig. 3D) (*25*). Peptide 25, but not a scrambled version of this peptide, inhibited the interaction of suPAR with Mac-1 (Fig. 3D). Peptide 25 (100 μM) also blocked the adhesion of phorbol 12-myristate 13-acetate (PMA)–stimulated myelomonocytic cells to vitronectin (*4*). These results directly parallel our observations with β1-integrins in 293 cells (Figs. 2 and 3) and confirm that activated integrins are a target for direct interaction with and regulation by uPAR.

We conclude that uPAR interacts with and modifies the function of integrins. This interaction both promotes adhesion to and migration toward a specific matrix protein, vitronectin, and suppresses the normal adhesive function of the integrins. Our results support a model in which uPAR both interacts via its extracellular domain with integrins that are in the active conformation, and makes use of the active conformer to connect to the cytoskeleton and mediate adhesion. The requirement for the GPI anchor for adhesion reflects the importance of this moiety in promoting the formation of stable uPAR-integrin-caveolin complexes, which might also serve to juxtapose distinct signaling and cytoskeletal elements associated with integrins and caveolin (*1*, *13*). These complexes provide a basis for dynamic cross talk between uPAR and integrins that might regulate integrin function both directly (by complex formation) and indirectly (by signaling). The proposed model could explain the previously described association of uPAR and urokinase with focal adhesions and with leading edges of migrating cells, the similarity of the properties of mechanical force transmission by uPAR and integrins, and the demonstration of signaling by uPAR (*3*, *6*, *26*).

Both increased expression of uPAR and loss of stable cellular adhesion have been linked to malignant transformation, tumor cell invasion, and metastasis in several experimental and clinical situations (*3*, *27*, *28*). In these instances, according to the proposed model, overexpression of uPAR might explain, in part, alterations in integrin function and cell adhesion. Destabilization of integrin-dependent adhesion by uPAR in vivo may also be promoted by the ability of uPAR to focus proteolytic activity to the cell surface (*3*). Indeed, the multiple concurrent engagements induced by uPAR suggest that this GPI-linked protein acts as an organizing agent to coordinate the migratory and invasive properties of cells. The role of other GPI-linked receptors that participate in adhesive interactions may be similar (*29*). The effects of uPAR on integrin function described here also suggest that reagents based on the peptide that alters integrin function by disrupting uPAR-integrin associations, or reagents comparable to soluble uPAR that impair integrin function, represent potential therapeutic agents for modifying inflammation and tumor progression.

REFERENCES AND NOTES

1. R. O. Hynes, *Cell* **69**, 11 (1992); C. H. Damsky and Z. Werb, *Curr. Opin. Cell Biol.* **4**, 772 (1992); S. J. Shattil, M. H. Ginsberg, J. S. Brugge, *ibid.* **6**, 695 (1994); M. E. Hemler, *Annu. Rev. Immunol.* **8**, 365 (1990); M. A. Schwartz, M. D. Schaller, M. H. Ginsberg, *Annu. Rev. Cell. Dev. Biol.* **11**, 549 (1995).
2. M. S. Diamond and T. A. Springer, *Curr. Biol.* **4**, 506 (1994); R. Li *et al.*, *J. Cell Biol.* **129**, 1143 (1995); X. P. Du *et al.*, *Cell* **65**, 409 (1991); T. A. Yednock *et al.*, *J. Biol. Chem.* **270**, 28740 (1995).
3. F. Blasi, J. D. Vassalli, K. Dano, *J. Cell Biol.* **104**, 801 (1987); E. Bacharach, A. Itin, E. Keshet, *Proc. Natl. Acad. Sci. U.S.A.* **89**, 10686 (1992); A. Estreicher, J. Muhlhauser, J. L. Carpentier, L. Orci, J. D. Vassalli, *J. Cell Biol.* **111**, 783 (1990); M. S. Pepper *et al.*, *ibid.* **122**, 673 (1993); W. Schlechte, G. Murano, D. Boyd, *Cancer Res.* **49**, 6064 (1989).
4. D. A. Waltz and H. A. Chapman, *J. Biol. Chem.* **269**, 14746 (1994); D. A. Waltz, L. Z. Sailor, H. A. Chapman, *J. Clin. Invest.* **91**, 1541 (1993); A. R. Nusrat and H. A. Chapman, *ibid.* **87**, 1091 (1991).
5. Y. Wei *et al.*, *J. Biol. Chem.* **269**, 32380 (1994). Neither 293 cells nor uPAR transfectants express measurable amounts of urokinase, and adhesion to vitronectin and fibronectin is not affected by aprotinin (Sigma).
6. J. Pollanen *et al.*, *J. Cell Biol.* **104**, 1085 (1987); G. Conforti, C. Dominguez-Jimenez, E. Ronne, G. Hoyer Hansen, E. Dejana, *Blood* **83**, 994 (1994); W. Xue, A. L. Kindzelskii, R. F. Todd III, H. R. Petty, *J. Immunol.* **152**, 4630 (1994).
7. J. Bohuslav *et al.*, *J. Exp. Med.* **181**, 1381 (1995); A. L. Kindzelskii, Z. O. Laska, R. F. Todd III, H. R. Petty, *J. Immunol.* **156**, 297 (1996); R. G. Sitrin *et al.*, *J. Clin. Invest.* **97**, 1942 (1996); D. I. Simon *et al.*, *Blood*, in press.
8. Cells in suspension were incubated with PI-PLC (1 U/ml) (Sigma) for 2 hours at 37°C. Cells were washed to remove soluble uPAR and then plated onto vitronectin- or fibronectin-coated surfaces in the presence of additional PI-PLC for a 1-hour adhesion assay as described (*5*).
9. Cells (5×10^5) were exposed to trypsin, incubated in suspension at 37°C for 1 hour and then with antibodies to β1-integrin or to uPAR on ice for 30 min, washed, and then incubated with either phycoerythrin-conjugated goat antibodies to rat immunoglobulin G (IgG) or fluorescein isothiocyanate–conjugated goat antibodies to mouse IgG (Sigma) as secondary antibodies for the rat and mouse primary antibodies, respectively. Cells were isolated by centrifugation, resuspended, and analyzed on a flow cytometer (FACScan; Becton Dickinson). Propidium iodide was added to allow determination of the proportion of permeable cells.
10. M. E. Lukashev, D. Sheppard, R. Pytela, *J. Biol. Chem.* **269**, 18311 (1994). Previously characterized stable clones of Ch1 and Ch2 transfectants were transfected with GPI-uPAR cDNA, and polyclonal mixtures of the resulting cotransfectants were assayed for adhesiveness to vitronectin.
11. Cells (5×10^6) were cultured overnight, washed twice with microtubule stablization buffer [0.1 M Pipes (pH 6.9), 2 M glycerol, 1 mM EGTA, 1 mM magnesium acetate], and then extracted on ice for 5 min in buffer containing 0.2% Triton X-100, 1 mM sodium orthovanadate, 1 mM phenylmethylsulfonyl fluoride, and leupeptin (10 mg/ml). The insoluble residue was solubilized at 4°C for 20 min in 1× RIPA buffer [150 mM NaCl, 50 mM tris-HCl (pH 7.5), 1% deoxycholate, 0.1% SDS, 1% Triton X-100] supplemented with protease inhibitors [R. L. Klemke, M. Yebra, E. M. Bayna, D. A. Cheresh, *J. Cell Biol.* **127**, 859 (1994)]. The original soluble fraction was diluted (1:1) with 2× RIPA buffer. Both fractions were centrifuged for 10 min at 2900*g*, and the supernatants were preincubated with nonimmune serum and protein A–agarose for 2 hours at 4°C. After centrifugation, the supernatants were transferred to fresh tubes and incubated with antibodies to β1-integrin or to caveolin (Transduction Laboratories) for 2 hours at 4°C. Washed immunoprecipitates were subjected to 8% SDS–polyacrylamide gel electrophoresis, and the separated proteins were transferred to a nitrocellulose membrane. The membranes were incubated with 5% (w/v) nonfat dried milk and then probed with R2 monoclonal antibodies to uPAR (1 μg/ml). The blots were washed and then incubated with horseradish peroxidase–conjugated goat antibodies to mouse IgG for 1 hour. After further washing, immune complexes were detected by enhanced chemiluminescence (DuPont Biotechnology Systems). Identical experiments were also performed with cells labeled with [^{35}S]methionine and [^{35}S]cysteine, and the immunoprecipitates examined by autoradiogaphy.
12. The full-length cDNAs encoding human uPAR and human IL-2Rα were isolated from macrophages and T cells, respectively, by reverse transcription and the polymerase chain reaction (*5*). A chimeric cDNA construct encoding the extracellular domains of uPAR (amino acids 1 to 281) and the transmembrane and cytoplasmic domains of IL-2Rα (amino acids 218 to 251) was prepared (TM-uPAR). The chimeric cDNA was subcloned into pBluescript, verified by nucleotide sequencing (Sequenase; United States Biochemical), digested with Xba I and Xho I, and then subcloned into the pCEP4 expression vector. As judged by immunoblot analysis and binding of vitronectin and urokinase, the levels of expression of GPI-uPAR and TM-uPAR in the stable transfectants were equivalent. TM-uPAR has been shown to bind urokinase normally [H. Li *et al.*, *J. Biol. Chem.* **269**, 8153 (1994)].
13. A. Stahl and B. M. Mueller, *J. Cell Biol.* **129**, 335 (1995); M. P. Lisanti *et al.*, *ibid.* **126**, 111 (1994); S. Li *et al.*, *J. Biol. Chem.* **270**, 15693 (1995).
14. R. J. Goodson, M. V. Doyle, S. E. Kaufman, S. Rosenberg, *Proc. Natl. Acad. Sci. U.S.A.* **91**, 7129 (1994); S. Fong *et al.*, in preparation.
15. Conditioned media from 293 cells expressing recombinant suPAR and control 293 cells were prepared as described (*5*). The concentration of suPAR in the conditioned medium was 67 nM as judged by enzyme-linked immunosorbent assay (American Diagnostica). Baculovirus-derived recombinant suPAR (20 to 100 nM) was also used to confirm all results obtained with suPAR-conditioned medium.
16. Human 293 cells (2.5×10^4) were seeded into Transwell (Costar) inserts containing 8-μm polycarbonate filters precoated on the bottom with fibronectin or vitronectin (10 μg/ml), and then cultured overnight in serum-free medium containing bovine serum albumin (BSA) (5 mg/ml). Cells on both sides of the filter were detached by trypsin-EDTA and counted.

All assays were performed in triplicate and the data expressed as the fraction of total cells appearing on the bottom of the filter.
17. Migration of low passage (1 to 3) human saphenous vein smooth muscle cells was assessed as described (*16*). Cellular spreading was assessed by phase-contrast microscopy of cells after 15 to 30 min at 37°C in microtiter wells coated with fibronectin or BSA. At least 200 cells were counted and the fraction remaining rounded was expressed as a percentage of the total.
18. R. I. Clyman, F. Mauray, R. H. Kramer, *Exp. Cell Res.* **200**, 272 (1992); M. P. Skinner, E. W. Raines, R. Ross, *Am. J. Pathol.* **145**, 1070 (1994).
19. Fibronectin binding was measured as described (*5*), and nonspecific binding in the presence of 0.5 mM RGD was determined to be <50% of total binding.
20. A. Masumoto and M. E. Hemler, *J. Biol. Chem.* **268**, 228 (1993).
21. D. I. Simon, A. M. Ezratty, S. A. Francis, H. Rennke, J. Loscalzo, *Blood* **82**, 2414 (1993). ^{125}I-Labeled fibrinogen (1 μM) was added to adenosine diphosphate–stimulated THP-1 cells (10^6) for 4 hours at 37°C. After addition of ice-cold 10% (w/v) trichloroacetic acid, the incubation mixture was centrifuged and soluble radioactivity was assayed as an index of fibrinogen binding and turnover. Nonspecific degradation was determined in the presence of a 50-fold molar excess of unlabeled fibrinogen. In this assay, THP-1 cells specifically degrade ~1 μg of fibrinogen per hour per 10^6 cells, which is inhibitable by >90% on addition of the LMP19c antibody to Mac-1. KIM 127, in the absence of suPAR, stimulated fibrinogen turnover by ~50%.
22. M. K. Robinson *et al.*, *J. Immunol.* **148**, 1080 (1992).
23. Full-length human Mac-1 was purified from a stably transfected 293 cell line expressing recombinant Mac-1. Detergent-extracted rMac-1 was purified on a lentil-lectin column followed by Q-Sepharose chromatography. The purity of the protein, determined by SDS-PAGE, was >85% (S. C. Bodary *et al.*, in preparation).
24. M. S. Diamond and T. S. Springer, *J. Cell Biol.* **120**, 545 (1993).
25. Microtiter plates were coated with recombinant Mac-1 (250 ng/ml) and then exposed to BSA (5 mg/ml). Biotinylated suPAR was added to each well in a solution containing 20 mM Hepes (pH 7.4), 150 mM NaCl, 1 mM $MnCl_2$, and 0.05% Tween 20, and the plates were incubated for 90 min at 25°C. After washing, bound suPAR was quantified with avidin-peroxidase as described (*5*). Binding to wells coated with BSA alone accounted for <20% of the total binding. suPAR bound to Mac-1 in a concentration-dependent manner over the range 0 to 250 nM. To assess the effect of Mac-1 activation on suPAR binding, we substituted 5 mM $CaCl_2$ and 5 mM $MgCl_2$ for 1 mM $MnCl_2$ in the binding solution.
26. N. Wang, E. Planus, M. Pouchelet, J. J. Fredberg, G. Barlovatz-Meimon, *Am. J. Physiol.* **268**, C1062 (1995); N. K. Rao, G. P. Shi, H. A. Chapman, *J. Clin. Invest.* **96**, 465 (1995); N. Busso, S. K. Masur, D. Lazega, S. Waxman, L. Ossowski, *J. Cell Biol.* **126**, 259 (1994).
27. C. W. Crowley *et al.*, *Proc. Natl. Acad. Sci. U.S.A.* **90**, 5021 (1993); H. Pedersen *et al.*, *Cancer Res.* **54**, 4671 (1994); E. Bianchi *et al.*, *ibid.*, p. 861.
28. S. A. Burchill, *BioEssays* **16**, 225 (1994); M. J. Weber, A. H. Hale, L. Losasso, *Cell* **10**, 45 (1977); T. David-Pfeuty and S. J. Singer, *Proc. Natl. Acad. Sci. U.S.A.* **77**, 6687 (1980).
29. M. C. Tiverson *et al.*, *J. Cell Sci.* **107**, 1783 (1994); R. H. Brakenhoff *et al.*, *J. Cell Biol.* **129**, 1677 (1995); C. L. Hall *et al.*, *Cell* **82**, 19 (1995).
30. Abbreviations for the amino acid residues are as follows: A, Ala; E, Glu; F, Phe; G, Gly; H, His; I, Ile; L, Leu; M, Met; N, Asn; P, Pro; Q, Gln; S, Ser; T, Thr; and Y, Tyr.
31. Supported by NIH grants HL44712 (to H.A.C.), HL 02768 (to D.I.S.), and HD 26732 (to Caroline Damsky) and a grant from the American Heart Association (to D.I.S.). We thank L. Gu for technical assistance, N. Rao for helpful discussions, E. Ronne for antibodies to uPAR, M. Robinson for KIM 127, and P. Libby for vascular smooth muscle cells.

5 April 1996; accepted 29 July 1996

Ecological Determinants of Species Loss in Remnant Prairies

Mark K. Leach and Thomas J. Givnish

Recensuses of 54 Wisconsin prairie remnants showed that 8 to 60 percent of the original plant species were lost from individual remnants over a 32- to 52-year period. The pattern of species loss was consistent with the proposed effects of fire suppression caused by landscape fragmentation. Short, small-seeded, or nitrogen-fixing plants showed the heaviest losses, as did species growing in the wettest, most productive environments. The interruption of landscape-scale processes (such as wildfire) by fragmentation is an often overlooked mechanism that may be eroding biodiversity in many habitats around the world.

Prairies covered 800,000 ha in Wisconsin before European settlement, but today they occupy less than 0.1% of their former extent and are mainly restricted to small, isolated remnants in a fire-suppressed landscape (*1*, *2*). Current theory predicts that each remnant should lose several plant species by habitat fragmentation. Because it alters the size, spacing, and context of individual habitat patches, fragmentation may increase the local rate of extinction by reducing population sizes or colonization from similar habitats (*3*–*5*), by eliminating keystone predators or mutualists (*6*, *7*), by exacerbating stochastic phenomena and genetic bottlenecks (*8*), or by changing the physical or biological environment through edge effects (*9*). The highest extinction rates are expected in species that are initially rare (*3*, *4*, *10*), that are geographically restricted (*10*, *11*), that require large unbroken patches of habitat or short distances between such patches (*5*, *9*), that rely on specialized pollinators or other mutualists (*6*, *7*, *10*), or that are competitive dominants with limited dispersal ability (*12*). However, such predictions ignore the effects of fragmentation on landscape-scale processes, such as wildfire, that affect the disturbance regime within individual patches (*13*). We propose that such effects are a dominant source of plant species loss in prairie remnants in the central United States; that they lead to disproportionate losses in short-statured, N-fixing, and small-seeded species; and that such losses are greatest in the most productive environments. We support these predictions by using a unique data set on species occurrences in prairie remnants, which display a remarkable rate of local plant extinction of 0.5 to 1.0% per annum over a 32- to 52-year period.

In the upper midwestern United States, frequent fire was the primary disturbance maintaining the open nature of prairies and oak savannas before European settlement, selecting against woody plants and favoring fire-adapted grasses and forbs (*1*, *2*). Once ignited by Amerindians or lightning (*1*, *2*), such fires were able to burn for many kilometers before being stopped by natural barriers (such as streams, swamps, and topographic breaks) or quenched by rain. For a given climate and soil, the area and local frequency of fires should increase with the area and contiguity of flammable terrain; the greater the area devoid of fire barriers, the more extensive each fire should be, increasing the average fire frequency at each point (*13*). After European settlement, we believe that local fire frequencies were reduced (*14*) not only by overt suppression, but also by fragmentation of a fire-prone landscape by nonflammable barriers such as roads and agricultural fields. By the 1940s and 1950s, most prairies in Wisconsin had disappeared except in certain fire-prone refugia (*1*, *2*, *15*), including railroad rights-of-way (where, before the 1950s, sparks cast by steam locomotives frequently started fires) and steep slopes with thin soils (where tilling was precluded and farmers had often grazed livestock and set fires in spring to encourage a new flush of growth). A few prairie remnants also persisted in country cemeteries, where infrequent mowing may have substituted for fire or grazing by native ungulates. Plant species lists of some 200 prairie remnants were compiled by Curtis and his colleagues (*1*) during the 1940s and early 1950s.

During and after the 1950s, the frequency of fire in railroad and hillside prairie remnants declined abruptly as human sources of ignition (steam locomotives and grazing of livestock on low-productivity slopes) were withdrawn in the context of a highly fragmented prairie landscape. We predict that, as a consequence, several

Department of Botany, University of Wisconsin, Madison, WI 53706, USA.